Geogr. Fis. Dinam. Quat.
45 (2022). 197-210, 11 figg., 3 tabb.

DOI 10.4461/ GFDQ.2022.45.8

FABRIZIO TROILO [1,4*], LUCA MONDARDINI [1], PAOLO PERRET [1], VALERIO SEGOR [2], DANIELE GIORDAN [3], NICCOLÒ DEMATTEIS [3] & FRANCESCO ZUCCA [4]

PERIGLACIAL CASCADING PROCESS IN AN ALPINE ENVIRONMENT: AN EXAMPLE OF AN ICE AVALANCHE-INDUCED DEBRIS FLOW IN FERRET VALLEY (COURMAYEUR, ITALY)

ABSTRACT: TROILO F., MONDARDINI L., PERRET P., SEGOR V., GIORDAN D., DEMATTEIS N. & ZUCCA F., *Periglacial cascading process in an alpine environment: an example of an ice avalanche-induced debris flow in Ferret Valley (Courmayeur, Italy).* (IT ISSN 0391-9838, 2022).

On 23 June, 2022, a debris flow occurred in the Montitaz Stream (Mont Blanc area), which flows off the Planpincieux Glacier snout. It destroyed the bridge that links the hamlets of Planpincieux and Rochefort. Using a multi-source dataset from UAV, satellite and terrestrial sensors belonging to the Planpincieux Glacier monitoring network, we reconstructed the series of events that led to the debris flow. We found evidence that this resulted from a cascading process which started with an ice avalanche of 4200 m^3 falling over a reformed glacieret that lies 500 m downstream from the glacier front. Subsequently, the deposited ice avalanche formed an unstable ice dam along the Montitaz Stream riverbed, causing a mixed accumulation of water and ice debris. Finally, the dam collapsed, originating a debris flow consisting of ice, water and debris from the glacial fan. DEM differencing showed that approximately 14,000 m^3 of material were mobilised overall.

KEY WORDS: Cascading process, Ice avalanche, Debris flow, Glacier monitoring, Remote sensing.

RIASSUNTO: TROILO F., MONDARDINI L., PERRET P., SEGOR V., GIORDAN D., DEMATTEIS N. & ZUCCA F., *Sequenza di processi periglaciali in ambiente alpino: un esempio di debris flow indotto da valanga di ghiaccio nella Val Ferret (Courmayeur, Italia).* (IT ISSN 0391-9838, 2022).

Il 23 giugno 2022, una colata detritica ha interessato l'alveo del Torrente Montitaz (Massiccio del Monte Bianco), il quale ha origine dalla fronte del Ghiacciaio di Planpincieux, distruggendo il ponte che collega il Villaggio di Planpincieux con il Villaggio di Rochefort. Grazie all'utilizzo di una serie di dati telerilevati da piattaforme satellitari, da sistemi UAV e da sensori terrestri appartenenti alla rete di monitoraggio del Ghiacciaio di Planpincieux, abbiamo potuto ricostruire una serie di eventi e di caratteristiche interconnesse fra loro, ricostruendo la sequenza di eventi che ha generato la colata detritica. In questo modo abbiamo scoperto che la colata detritica rappresenta la parte finale di una serie di processi a cascata innescati da un crollo di ghiaccio di circa 4200 m^3, la conseguente valanga di ghiaccio che ha raggiunto il sottostante ghiacciaio nevato del Montitaz (a circa 500 m di dislivello a valle della fronte del ghiacciaio di Planpincieux), sovrascorrendolo e formando un deposito di detriti di ghiaccio nell'alveo del Torrente Montitaz, formando una diga effimera e conseguentemente uno sbarramento al deflusso che ha causato un accumulo di acqua e ghiaccio. Il collasso dello sbarramento effimero ha poi originato la colata detritica, prendendo in carico detrito dal conoide glaciale. L'analisi multi temporale dei dati topografici ha dimostrato infine che circa 14 000 m^3 di materiali sono stati mobilizzati durante l'evento.

TERMINI CHIAVE: Processi a cascata, Valanga di ghiaccio, Colata di detrito, Monitoraggio di ghiacciai, Telerilevamento.

[1] *Fondazione Montagna Sicura, Glaciers snow and avalanche research area, Courmayeur, Italy.*

[2] *Regione Autonoma Valle d'Aosta, Mountain basins geo-hydrological department, Aosta, Italy.*

[3] *Research Institute for Geo-Hydrological Protection IRPI, Italian National Research Council, Torino, Italy*

[4] *University of Pavia, Department of Earth and Environmental Sciences, Pavia, Italy.*

** Corresponding author: F. Troilo (ftroilo@fondms.org)*

The authors would like to thank all the staff of the Fondazione Montagna sicura which supports the research activities of the research team, and the administration of the Autonomous Region of Aosta Valley for its continuous support to the Fondazione Montagna sicura especially in regards to the Coordinator of the reference department Ing. Raffaele Rocco and the General Secretary of Fondazione Montagna sicura Dr. Jean-Pierre Fosson. We would like to thank Dr. Ethienne Berthier from CNRS - LEGOS (Laboratoire d'Etudes en Géophysique et Óceanographie Spatiales) for supporting us with useful informations and test datasets in the prospective phase of the acquisition and processing of satellite stereo imagery. The authors would like to thank Prof. Martin Funk for supporting with great passion and dedication the research and monitoring activities in the field of glacial risk as a member of the scientific comeetee of the Fondazione Montagna sicura. The acquisition of the Pleiades Stereo image pair taken on the 4 September, 2020 was founded by the project Interreg Alcotra 2014-2020 (IT-FR) "RESERVAQUA" co-financed cross boarded project.

INTRODUCTION

Glacier-related hazards are a major issue for mountain communities, moreover exacerbated in the context of climate change. Rapidly evolving glaciers (Zemp & *alii*, 2021) can lead to the formation of unstable glacial lakes or snouts that can evolve in dangerous processes like Glacial Lake

Outburst Floods (GLOF) (Carrivick & Tweed, 2016; Emmer, 2017; Harrison & *alii*, 2018; Schneider & *alii*, 2014) and ice avalanches (Pralong & Funk, 2006). Furthermore, gravitational processes involving solid or liquid phases or a combination of those (Cicoira & *alii*, 2022) can have longer runouts than single-phase processes (Mergili & *alii*, 2020). Therefore, they can easily reach the bottom of slopes and be potentially dangerous for alpine settlements, infrastructures and people (Carrivick & Tweed, 2016; Huggel & *alii*, 2013; Kääb & *alii*, 2005). Complex phenomena involving different phases and interactions, known as cascading processes (Emmer & *alii*, 2022; Mazzorana & *alii*, 2019), pose a challenge in understanding mountain processes and individuation of early warning and monitoring solutions of such potentially destructive hazards. Examples of such processes have been recently documented at Piz Cengalo in Switzerland (Mergili & *alii*, 2020) and in the Chamoli region in Uttarakhand district in India (Pandey & *alii*, 2022), where highly destructive impacts on the anthropised valley floors were noticed. Cascading events are often very dangerous because the processes that compose these events can evolve or occur in different conditions compared to the ones that are typical for single processes (Cicoira & *alii*, 2022). The case under consideration is a typical example in which a debris flow occurred in a period not characterised by heavy rainfalls, involving thus the possibility that a more complex process had triggered the event.

In this paper, we describe a cascading process occurred on 23 June, 2022 in Ferret Valley, Italy. The process started as an ice avalanche from the unstable glacier front (Cuffey & Paterson, 2010) of the Planpincieux Glacier (Dematteis & *alii*, 2021). The ice deposited in the lower Montitaz stream and partially blocked its flow. The unstable dam of ice deposits collapsed, causing a dam brake outburst flood. A mixture of ice, water and debris reached the road crossing the stream and destroyed the bridge isolating the village of Rochefort in the Courmayeur municipality. We reconstructed the dynamics of the cascading process using high-rate terrestrial systems, UAVs, and different spaceborne sensors such as Airbus Pleiades stereo imagery and Sentinel-2 and Planetscope multispectral data.

STUDY AREA

This study analyses the cascading process which occurred on 23 June, 2022 in the Montitaz Stream (UTM-WGS84 coord: E: 343014,74; N: 5077657,13; elev: 1700 m) – Ferret Valley, Courmayeur Municipality, Italy – along the road that links the hamlets of Planpincieux and Rochefort (fig. 1).

The Montitaz Stream is a small tributary of the Dora di Ferret River and originates from the right lobe (i.e., Montitaz Lobe) of the Planpincieux Glacier, at ~2650 m. It's fed by the glacier melting in the warm season, while in the cold season, its flow almost dries up. The course of the Montitaz is composed of three sections: i) above the altitude of 2100 m, the stream flows directly on a 37° steep exposed bedrock and the thalweg is narrow (20-50 m). ii) Between 2100-1800 m, the Montitaz flows across a 21° steep glacial fan, composed of easily mobilized debris. ii) Below 1800 m, the slope is gentler and the stream morphology becomes of *rapid* type (sensu Halwas and Church (2002); the road between the villages of Planpincieux and Rochefort is situated at the beginning of this last section.

The Planpincieux Glacier (RGI60-11.02991) is a medium size (area: 1.013 km^2) glacier located in the Italian part of the Mont Blanc massif. The elevation ranges between 2650 m and 3680 m, its aspect is mostly south-east and the accumulation area is overlooked by rock faces from the Grandes Jorasses (4208 m). Smaller ice avalanches of a few thousand cubic meters are frequent during the warm season (Giordan & *alii*, 2020). Since 2013, the Planpincieux Glacier has been monitored by the Autonomous Region of Aosta Valley, the Fondazione Montagna Sicura and the Research Institute for Geo-hydrological Protection for the risk of collapse of a major part of the Montitaz Lobe (Dematteis & *alii*, 2021).

A lower glacial body – hereafter called Montitaz Glacieret – fed by the accumulation of ice avalanche deposits from the upper front of the Montitaz Lobe disappeared in 2015 and reformed in 2019 due to the increased ice fall activity. The glacieret lies at 2000-2100 m at the top of the glacial fan (i.e., at the beginning of the second sector formerly described of the Montitaz Stream). Its extension can vary in one single season, mainly during the melt season, as well as between different years as a balance of ice fall activity and the ablation during the warm season (fig. 2).

DATASETS AND MATERIALS

In this study, we adopted a multi-source dataset that includes the equipment belonging to the monitoring network of the unstable Planpincieux Glacier front and other data explicitly acquired to investigate the cascading process. The list of the adopted dataset is shown in tab. 1.

The monitoring network comprises a Doppler radar, which is dedicated to the detection of ice avalanches coming from the Montitaz Lobe. The Doppler radar is linked to traffic lights on the main road to stop traffic in case of event detection (Meier & *alii*, 2016).

An AXIS Q6315-LE PTZ dome camera is scheduled to acquire hourly images. In case of an event, the Doppler radar triggers a burst of one image per second.

A Ku-band ground-based synthetic aperture radar (GB-SAR) monitors the Montitaz Lobe 24/7. Terrestrial radar interferometry (TRI) (Caduff & *alii*, 2015; Monserrat & *alii*, 2014) provides displacement values every four minutes. Alarms are sent in case of strong accelerations of the glacial mass that could be forerunners of a major destabilisation and a subsequent large ice avalanche.

Two 18 MP DSLR time-lapse cameras (TLCs) acquire hourly images and provide displacement data of the Planpincieux Glacier at a daily frequency (Dematteis & *alii*, 2021) using digital image correlation technique (DIC) (Evans, 2000; Schwalbe & Maas, 2017). Moreover, the images are used to detect glacier morphological variations and -estimate released volumes of ice break-offs (Giordan & *alii*, 2020).

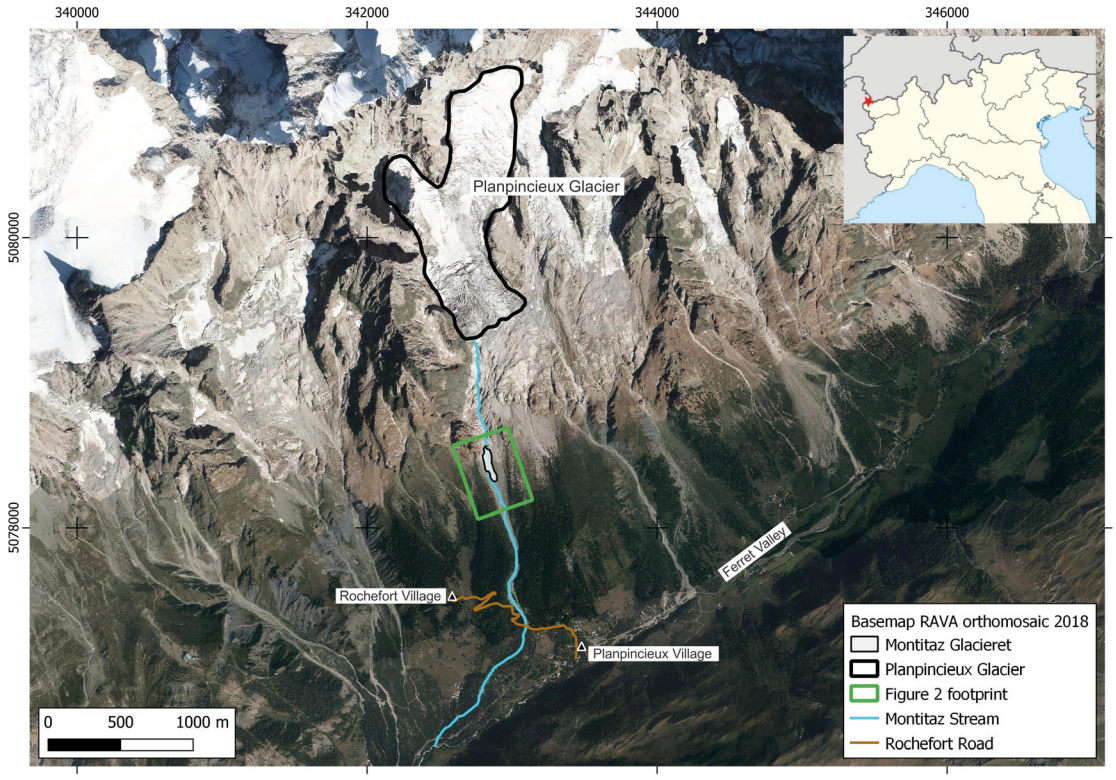

FIG. 1 - Location map of the study area. Detail of the Ferret Valley, the Planpincieux Glacier, the Montitaz Stream and the adjacent villages of Planpincieux and Rochefort. The Rochefort Road is highlighted: its crossing of the Montitaz Stream correspond to the area interested by the major impact of the debris flow studied in this paper.

FIG. 2 - View of the ice avalanche detached from the Planpincieux Glacier front and accumulated in the Montitaz Stream, between 1900 m and 2000 m a.s.l., at the base of the rocky slope downvalley the Planpincieux Glacier front. Note that the stream disappears and flows under the Montitaz Glacieret and re-emerge at the lower end of the glacieret. The photo was acquired in the morning after the debris flow event. Note the marks of flooding outside the stream (dark gray).

Doppler radar, AXIS camera and GBSAR are installed in the Planpincieux hamlet, while the TLCs are on the top of Mont de La Saxe, on the valley side opposite the Planpincieux Glacier. Furthermore, a webcam close to the bridge of the Planpincieux-Rochefort road acquires live video for surveillance.

In addition, we used available historical orthoimages and digital elevation models (DEMs) and an orthoimage and DEM acquired 5 days after the debris flow occurrence. These new acquisitions were conducted using an Autel Evo 2 Enterprise quadcopter equipped with a 20Mp digital camera (sensor width of 1"). 316 images were acquired during the survey with a resolution of 5472x3648 pixels and the geocoding was conducted in RTK mode, using 6 ground control points (GCPs) as support and a virtual base station of the SPIN GNSS (www.spingnss.it). The nearest station of the network is the "RUMI" station located at 21 km of distance and equipped with a LEIAR25.R4 LEIT antenna and a LEICA GR25 (GPS+GLO+GAL) receiver. Errors were estimated on 3 checkpoints of the photogrammetric model. A DEM of the higher area was also used to map the extent of an ice avalanche that occurred on 10 November, 2021. The DEM was built via Structure from Motion (SfM) from the image dataset acquired with a Mavic 2 Pro UAV, equipped with a Hasselblad digital camera shooting 20 MP images. The survey was performed without GCPs, but a DEM coregistration on the UAV-acquired DEM dating from 28 June, 2022, used as a reference, was carried out to obtain higher geocoding precision. The DEM had an original resolution of 0.13 m which was resampled to 2 m to match the Pleiades DEM resolution (see below). All co-registration procedures done in the present study have been performed with the implementation of the algorithm outlined by Nuth and Kaab (2011); for that purpose, we used python code freely avalaible at https://github.com/dshean/demcoreg#demcoreg. We opted for UAV survey on UAV RTK survey DEM coregistration and Stereo satellite on Aerial Lidar DEM for coherence in spatial resolution of the products. UAV RTK survey DEM and Aerial Lidar DEM showed very small altitudinal differences on stable terrain and thus did not need to undergo further coregistration.

A 3D georeferenced point cloud of the glacial front of the Planpincieux Glacier was used to estimate the release volume of the ice avalanche of 23 June, 2022. The acquisition of the digital images was performed with a digital camera (Nikon D850, dataset of 88 images of 8256x5504 pixel resolution) shotted onboard a helicopter on the day after the event in the frame of the regular surveys in the monitoring plan of glacial risk coming from the Planpincieux Glacier front. The georeferencing of the survey was made using 13 GCPs around the glacier snout (Dematteis & *alii*, 2021). Moreover, it was also possible to acquire pictures of the lower area of the Montitaz Stream with the same camera as above, such as the image in fig. 2. Pre-event DEM was built using AIRBUS Pleiades 0.5 m-resolution Stereo pair (Berthier & *alii*, 2014) dating from 04 September, 2020. The satellite stereo imagery produced a 2 m resolution DEM over the study area.

A GNSS field survey was carried out and 6 GCPs were measured on stable ground, to assess the accuracy of the elevation information coming from different datasets. The control points were distributed in the central part of the surveyed area. In contrast, the higher area could not be surveyed at the time of the event, as the road to access the upper area remained closed for a month after the destruction of the bridge. The GNSS survey was performed with a Geomax Zenith 25 Pro receiver adopting RTK corrections via a virtual reference station of the SPIN GNSS as for the drone images georeferencing. While in the UAV data processing, all 6 GCPs could be used (3 entered as control points and 3 as checkpoints), for the processing of the satellite images, only 3 GCPs could be used because of poor visibility of some of those in the native 0.5 m resolution imagery; those 3 GCPs were used as checkpoints.

We collected meteorological data from three automatic weather stations (AWSs) managed by the regional "Centro Funzionale" of the Aosta Valley Region (www.cf.regione.vda.it). The AWSs are located close to the area of study – Ferrachet (@5.5 km, E 346984 m, N 5081340 m, alt. 2290 m), La Saxe (@2 km, E 343313 m, N 5075894 m, alt. 2110 m) and Dolonne (@5 km, E 342036 m, N 5073422 m, alt. 1200 m) – and acquire hourly precipitation data.

Finally, we adopted freely avalaible ESA (European Space Agency) Sentinel-2 (T32TLR_20220623T103031, resolution 10 m) and commercial Planet Labs Inc. Planetscope (20220623_100014_41_2483_3B_AnalyticMS_SR_8b_harmonized, resolution 3 m) multispectral images. Such images were acquired the same day of the cascading process at h12:00 local time for the Planetscope imagery and h12:38 local time for the Sentinel-2 imagery (tab. 1).

METHODS

To reconstruct the complex dynamics of the cascading process, we operated a series of tasks using the available multi source data: i) we determined the general state of the system (glacier, glacieret and stream) before the event using historical orthoimages and DEMs acquired by UAV, satellite stereo imagery, oblique images acquired by the AXIS camera, and Normalised Difference Water Index (NDWI) (McFeeters, 1996) derived by Sentinel-2 and Planetscope multispectral images; ii) we analysed the meteorological conditions (cumulated precipitation and intensity) before and during the event; iii) we determined the precise timing of the debris flow occurrence using the survey webcam of the Planpincieux-Rochefort bridge; iv) we evaluated the state of activity of the glacier using displacement data from TRI and DIC, and we analysed time-lapse and AXIS images and doppler data to identify possible ice avalanches or GLOF; finally, v) we mapped the area involved in the debris flow and measured its volume using orthoimages and DEM differencing. The abovementioned steps of the workflow are summarized in fig. 3. The aerophotogrammetrical UAV survey of 28 June, 2022 and all other photogrammetrical surveys cited in the paper (i.e., ice avalanche deposit on 10 November, 2021; Planpincieux Glacier front on 24 June, 2022), were processed using SfM from Agisoft Metashape

TABLE 1 - Available monitoring systems, products and their use.

Monitoring system	Products	Application
Sentinel-2 satellite	Orthoimage NDWI	Site state before the event
Pleiades satellite	Stereo imagery Orthorectified image DEM	Site state before the event
Planetscope	Orthoimage NDWI	Site state before the event
UAV	Orthoimage DEM	Site state before and after the event Debris flow mapping Debris flow volume estimation
Aerial Lidar	DEM	DEM coregistration, Satellite image orthorectification Satellite image orthorectification
Aerial photogrammetry RTK GNSS	Orthoimage Ground control points	DEM error quantification
AXIS camera*	Hourly photographs	Site state before and after the event
Bridge survey webcam*	Live video	Timing of the event
AWS	Semi-hourly rainfall data	Environmental conditions
Doppler radar*	Ice avalanche detection	
GB-SAR*	Near-real time glacier displacement	State of glacier activity
TLCs*	Daily glacier displacement Hourly photographs	State of glacier activity Ice avalanche / GLOF occurrence

* These apparatuses belong to the monitoring network of the Planpincieux Glacier.

(Jebur & *alii*, 2018) software. The survey conducted on 28 June, 2022 was processed with 3 checkpoints for model error estimation and 3 control points for the model construction. A georeferenced dense cloud of 127 million points was produced; using this pointcoud, a 0.13 m/pixel ground resolution DEM and an orthomosaic with 0.065 m/pixel ground resolution were extracted.

In tab. 2, the coordinates of the reference points used in this study are reported, together with calculated errors on checkpoints both on the UAV and on the Pleiades DEMs, and finally, the difference between the two DEMs is also calculated on 3 checkpoints.

The AIRBUS Pleiades Stereo pair was processed using the Orthoengine tool of PCI GEOMATICA commercial software. We processed without GCPs, using orbital parameters only, with a second step of coregistration on stable areas, following procedures highlighted by (Nuth & Kääb, 2011), together with the regional 2 m DEM acquired by Aerial Lidar in 2008. An orthorectified image was also produced starting from one of the native stereo Pleiades images with the same software as above using the Aerial Lidar regional elevation data of 2008 and classic aerophotogrammetrical regional survey data of 2005 for the positioning of control points.

RESULTS

System conditions before the event

Fig. 4 shows the NDWI on 23 June, 2022 at h 10:30, which is higher along the thalweg of the Montitaz Stream above 2100 m, thus indicating a high probability of the presence of water, and below 2000 m, where the stream runs off the glacieret (reference fig. 2 and fig. 3). In correspondence with the Montitaz Glacieret, the NDWI shows a sharp decrease, thereby marking that water flowed underneath the ice deposit. The NDWI value is relatively small, but the relevance of the data consists more on the NDWI gradient along the profiles and the e spatial coherence in the gradients along the transect. It should also be considered that such a small stream cannot build up a strong signal with the ground resolution of the available sensors (10 m and 3 m).

The high temperatures of the period when the debris flow occurred caused significant ice melting. Even though we did not have available water discharge measurements, direct visual observations showed an abundant flow in the Montitaz Stream (fig. 4).

Meteorological conditions

Fig. 4 shows hourly precipitation data collected by the Ferrachet, Dolonne and La Saxe AWSs. The maximum total precipitation registered in the 24 hours before the debris flow was 6.5 mm, and approximately 90% of the cumulated precipitation fell between h 14:00 and h 15:00. Moreover, no rainstorms were registered in the study area on the day of the event (fig. 5).

Determination of the timing

We determined the precise debris flow timing from the video of the survey webcam installed close to the bridge of the Montitaz Stream. The impact of the debris flow on the bridge occurred at h 20:45 (fig. 6A2). During the event, the bridge was severely damaged (fig. 6A3-4).

TABLE 2 - Coordinates of reference points and calculated point coordinates for error estimation of the UAV and Pleiades DEMs as well as the differences between the two DEMs.

Ground Control Points			
GCP ID	Easting (m)	Northing (m)	Altitude (m)
102	342887.051	5076953.603	1592.725
104	342902.415	5076949.896	1591.316
106	342889.792	5076981.772	1595.100
108	342878.555	5077040.699	1600.800
109	343110.180	5077322.196	1674.938
111	343108.689	5077335.473	1678.649
Pleiades Stereo DEM errors			
Point ID	Easting errors (m)	Northing errors (m)	Altitude errors (m)
102	-0.198	-0.388	-0.282
106	0.458	-0.207	-0.062
108	-1.061	-0.710	-0.547
RMSE	0.677	0.482	0.357
UAV DEM errors			
Point ID	Easting errors (m)	Northing errors (m)	Altitude errors (m)
104	0.085	0.228	0.151
106	0.181	0.054	-0.010
109	-0.237	-0.342	0.169
RMSE	0.179	0.239	0.131
UAV 2m resampled DEM vs 2m Pleiades DEM Altitudinal differences			
Point ID	UAV altitude (m)	Pleiades altitude (m)	
102	1592.514	1593.007	0.493
106	1594.888	1595.162	0.274
108	1601.432	1601.444	0.012
RMSE			0.325

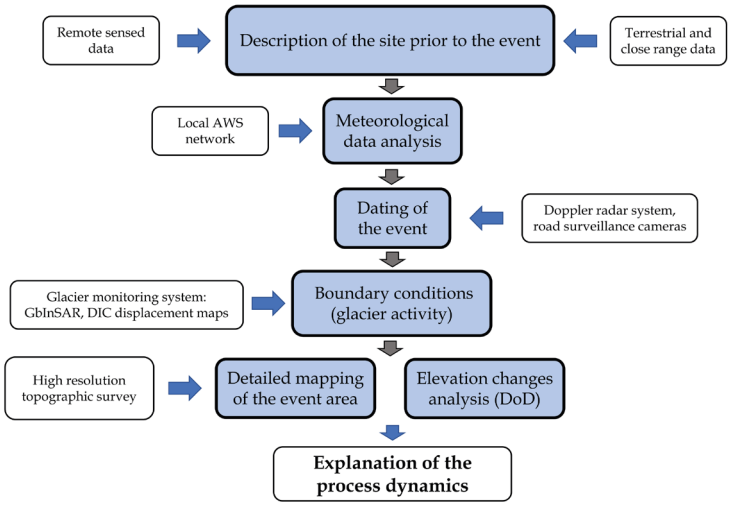

FIG. 3 - Workflow summarizing the methodology applied in this study for the reconstruction of the dynamics that caused the Montitaz Stream debris flow on 23 June, 2022.

State of the Planpincieux Glacier activity

The motion of an ice chunk at the glacier front markedly increased in the 3 days before the event. The GBSAR system detected an acceleration of the glacial front on 23 June, 2022, which culminated at around h 20:00, followed by a decrease in velocity, which is typical of a process of destabilisation, acceleration of the ice mass and subsequent collapse that generates an ice avalanche (Giordan & *alii*, 2020). Analogously, the acceleration was registered by the DIC results of the TLC, where the unstable portion was evident.

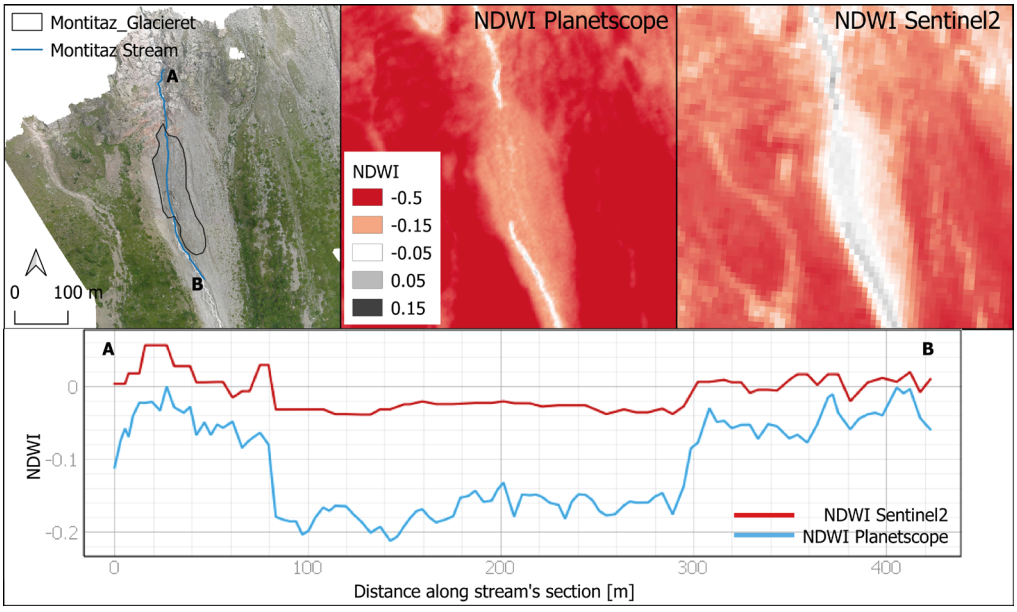

FIG. 4 - NDWI index maps obtained from Sentinel-2 and Planetscope imagery taken on the 23 June, 2022 (h 12:38 and h 12:00 local time, respectively). Water flowing into the Montitaz Stream is highlighted by higher NDWI values along the thalweg, while lower values characterise the area of the Montitaz Glacieret where the water disappears, flowing underneath the glacieret. ©Planet Labs PBC, CC BY-NC-SA 2.0.

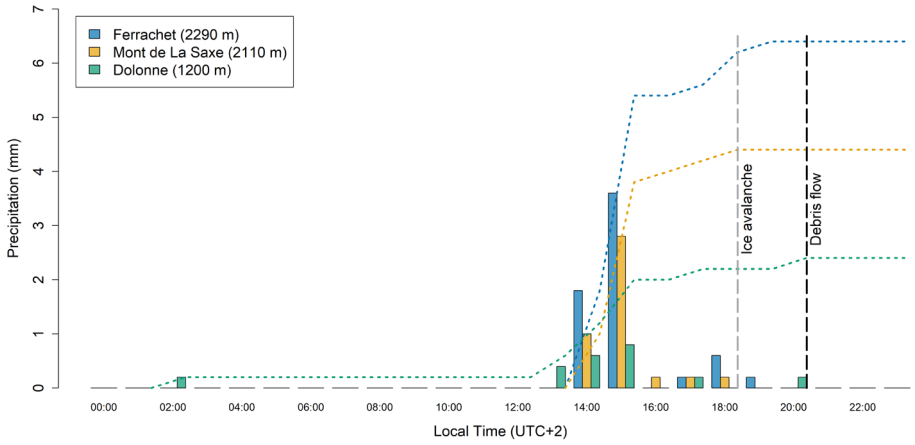

FIG. 5 - Pluviometric data from the Ferrachet, Dolonne and La Saxe AWS located in the Ferret Valley. Histogram refers to hourly precipitation, dashed blue yellow and green lines indicate cumulated precipitation of the single AWS. Vertical dashed grey and black lines indicate the timing of the ice avalanche and debris flow events.

Additionally, comparing the hourly time-lapse images, we identified an ice break-off that occurred between h 18:00 and h 19:00 (fig. 7A). The volume of 4500 ± 1500 m^3 involved in the ice fall has been performed by photogrammetric measures on the digital imagery from the TLC of the Planpincieux Glacier monitoring system (Giordan & *alii*, 2016). Due to the relatively high uncertainty of this methodology, a measurement of the ice fall scar has been made on data from the aerophotogrammetrical survey of the glacial front performed on the morning after the ice fall event. The ice fall scar could be easily located and confirmed by the confrontation of high-resolution time-lapse cameras before and after the event. The scar had a mean depth of 7 m, a width of 36.8 m and a mean ice thickness of 16.3 m, yielding a volume of 4200 m^3. With the positioning of natural reference points (homologous points on exposed bedrock found on TLC images and UAV images) for volume calculation in the order of ±20 cm on a very fine resolution (average point spacing 5 cm) georeferenced 3D point cloud, and the uncertainty of the exact geometry of the collapsed glacial front (we estimated its geometry by interpolation of the intact glacial front to the left and right of the ice fall scar) we estimate accuracy in the order of ±500 m^3. This confirmed good performance of the first estimation method, probably helped by the simple geometry of the ice chunk and the very well-defined ice fall scar. We took the volume estimation on the 3D model as a reference.

The downslope ice deposit was visible on an image acquired at h 19:00 by the AXIS camera and it accumulated a few tens of meters below the Montitaz Glacieret. Such images do not show evidence of a large accumulation of ice debris, but rather show a mixture of thin accumulation of small ice debris and flowing/erosional features on the glacieret surface (fig. 7B). Therefore, there is evidence that an ice avalanche impacted the glacieret and deposited in the Montitaz Stream approximately two hours before the debris flow reached the bridge downstream. Since the volume of the break-off was relatively small, the Doppler radar did not detect the avalanche; consequently, the AXIS camera did not acquire a concurrent high-rate image burst (fig. 7).

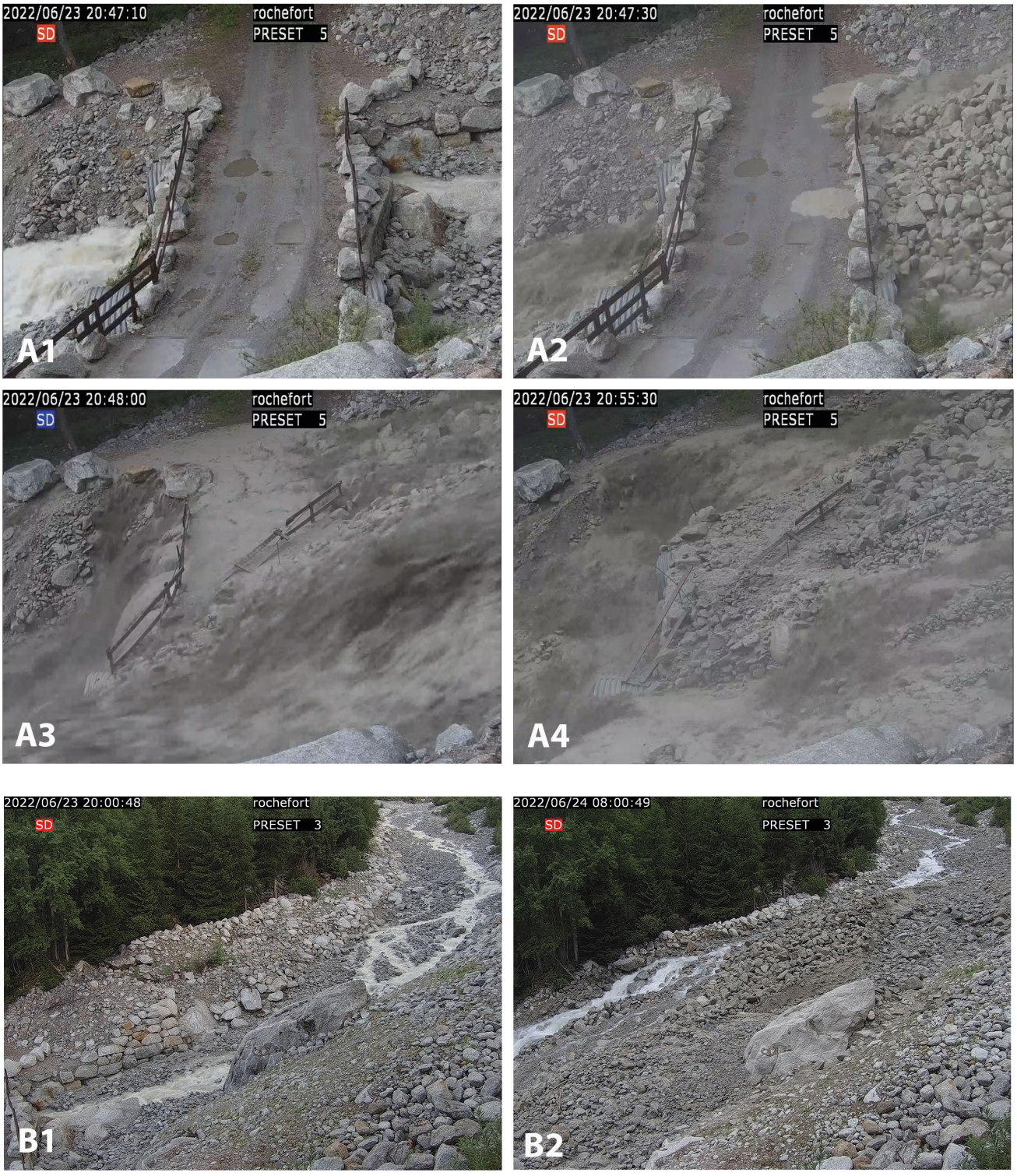

FIG. 6 - Sequence of images of the Rochefort bridge that crosses the Montitaz Stream. A1 to A4 are images of the camera surveying the bridge when the debris flow impacted the bridge h 20:47-h 20:55. B1 and B2 are images of the camera surveying the Montitaz Stream just above the bridge at h 20:00 before and at h 08:00 the morning after the event. A significant deposition of debris is evident.

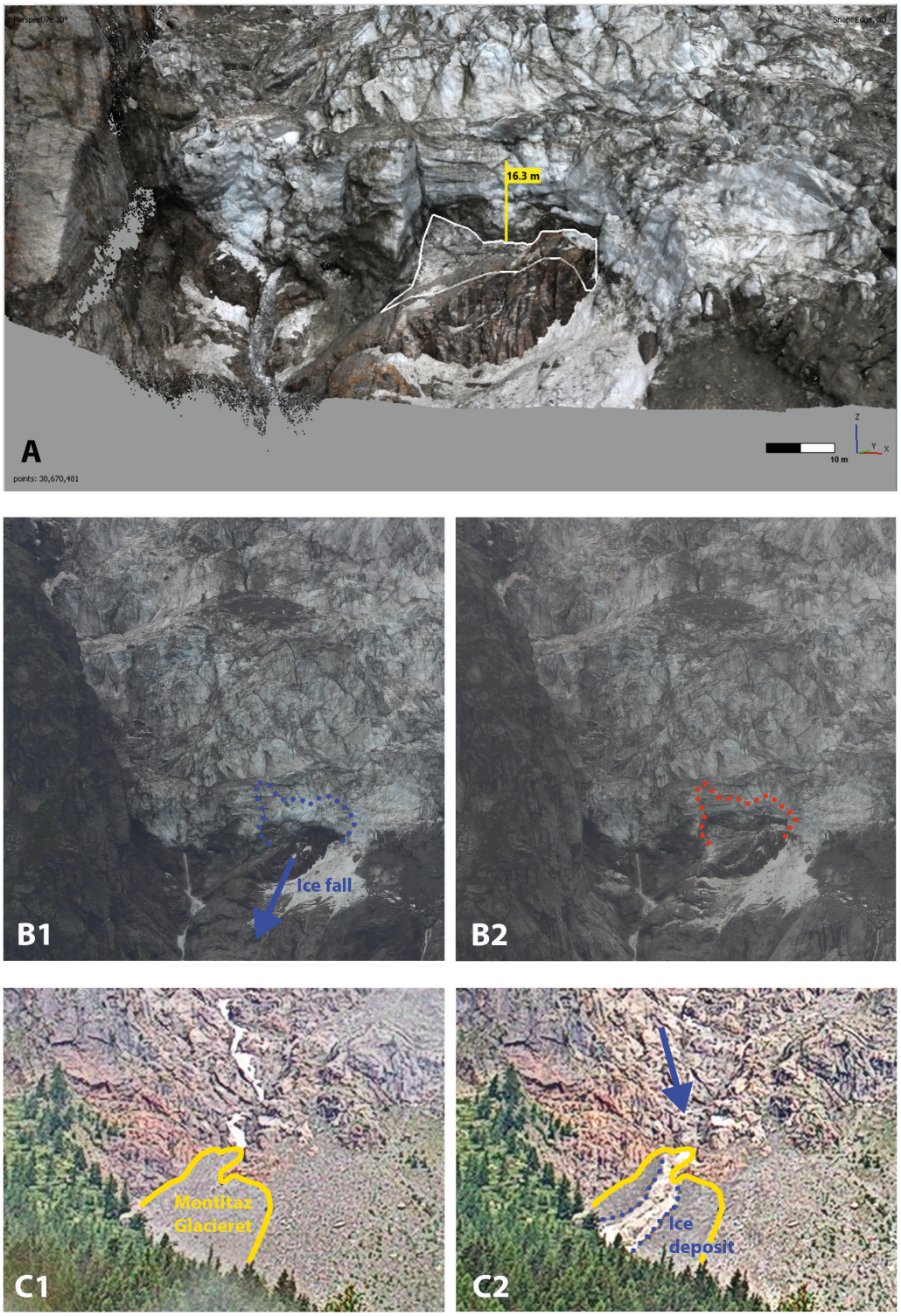

FIG. 7 - A) Individuation of the basal surface of the ice detachment on the georeferenced 3D point cloud of the Planpincieux glacier obtained by SfM processing and collapsed ice thickness measure. B1 and B2) Evidence of an ice fall from the front of Planpincieux Glacier on digital high-resolution time-lapse imagery from the 23 June, 2022 at h 18:00 and h 19:00. The collapsed volume was estimated to 4200 m^3 ± 500m^3. C1 and C2) AXIS camera images of the Montitaz Glacieret at C1 h 18:00 and C2 h 19:00. In C2, the ice deposit of the avalanche that had overflown the Montitaz Glacieret is highlighted.

Debris flow mapping and volume

The day after the event, a helicopter flight was carried out. Fig. 8 shows details that allow one to individuate the starting point of the debris flow. Fresh erosional features start to be present from 1940 m altitude on the right bank of the stream and from 1925 m on the left bank of the stream. An elongated patch of ice debris is located on top of the left margin of the stream at the same location of the first appearance of fresh erosional marks and reaching its maximum point of reach at around 1900 m. Such lateral elongated ice debris patches have already been observed on ice avalanche deposits coming from the Planpincieux Glacier and stopping in the Montitaz Stream (Mergili & *alii*, 2020).

Based on the abovementioned observations, we locate the probable deposition area of the ice avalanche that partially blocked the stream, causing the start of the mass movement, at an altitude between 1950 m and 1900 m (fig. 9).

The probability that the ice avalanche deposited in this area is also confirmed by past documented events having similar starting volumes and that have frequently had points of reach in the same area, such as the ice avalanche event of 10 November, 2021 depicted in fig. 8, which had an estimated release volume of 4900 ± 1600 m^3.

Five days after the event, a UAV survey was conducted to map the deposit and estimate the volume of the mobilised debris (fig. 10). Using a Dem of Difference (DoD) based on the confrontation of the 4 September, 2020 Pleiades DEM and the DEM acquired by UAV on 28 June, 2022, we were able to analyse the elevation changes that occurred following the event of 23 June, 2022 (tab. 3). We interpreted the elevation losses along the higher part of the stream as related to erosional processes linked to the event under analysis. Lower down the stream towards the Rochefort bridge crossing, we have instead interpreted the elevation gains as depositional features from the abovementioned event. In the accumulation area, elevation changes were matched by changes in the distribution and texture of the debris along the stream. Lateral elongated depositional features were present upstream, and a lower main body was identified just against the bridge. This main accumulation body is visible in the surveillance camera imagesin fig. 7B. The results of the DoD showed maximum thicknesses of the debris flow accumulation in this area as high as 6 m. In this way, it was possible to calculate eroded and deposited volumes that, with the introduction of the fallen ice mass that was remobilised and entrained in the gravitational process, reach similar values in the balance between eroded and accumulated volumes (fig. 10).

TABLE 3 - Description of the involved volumes in the gravitational process. A summary of estimated eroded volumes and deposited volumes of material linked to the event of 23 June, 2022. Negative volumes represent the missing volumes in the higher section of the stream comprised of the negative areas of the DoD available from pre and post event conditions that we interpret as eroded debris, and the ice volume that fell from the glacier front on 23 June, 2022 that was taken in the debris flow process and subsequently disappeared from the higher area of the Montitaz stream. Positive volumes are represented by areas of positive values in the pre and post event DoD in the lower section of the Montitaz stream.

Area type	Volume (m^3)	Accuracy (m^3)
Erosional (debris)	-4597	±1986
Erosional (Ice)	-4200	±500
Accumulation Ice+Debris	+13,533	±1530

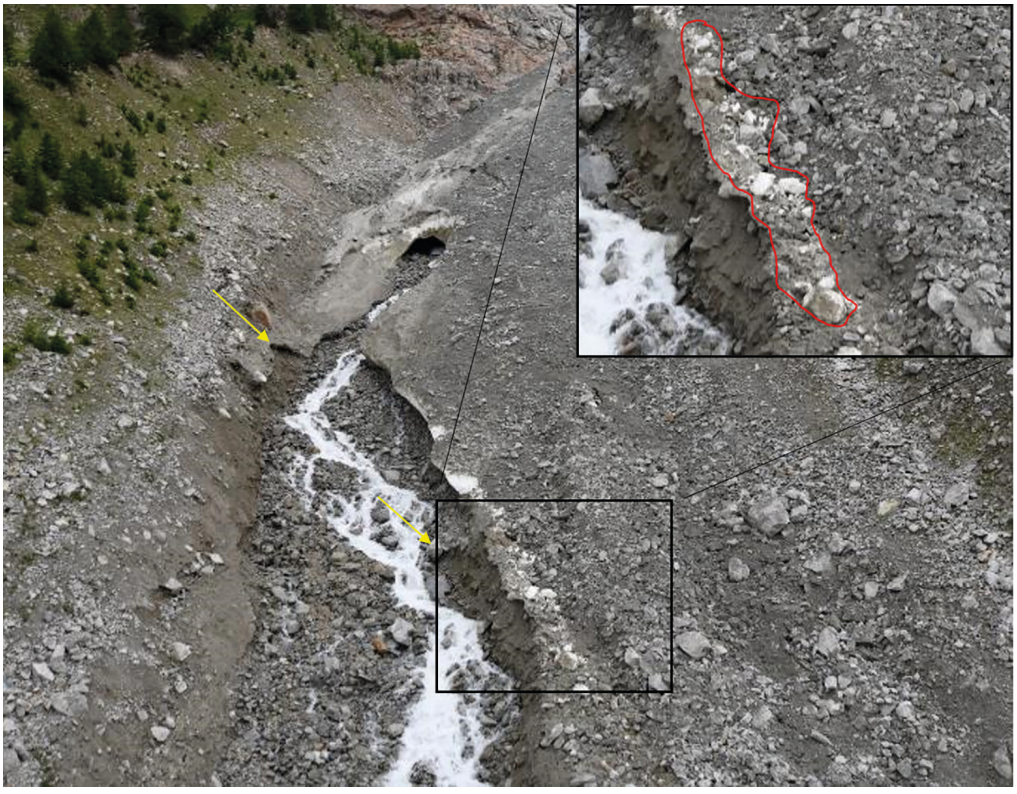

FIG. 8 - The starting points of the freshly activated erosional processes are visible on pictures from the helicopter survey carried out the morning after the debris flow event (i.e., 24 June, 2022, highlighted with yellow arrows). The ice avalanche deposit has almost completely been washed out or eroded, but a small elongated patch of ice debris is still in place on the left bank of the stream (upper right inset, red outline). The distance between the higher erosional feature and the ice debris patch is approximately 60 m.

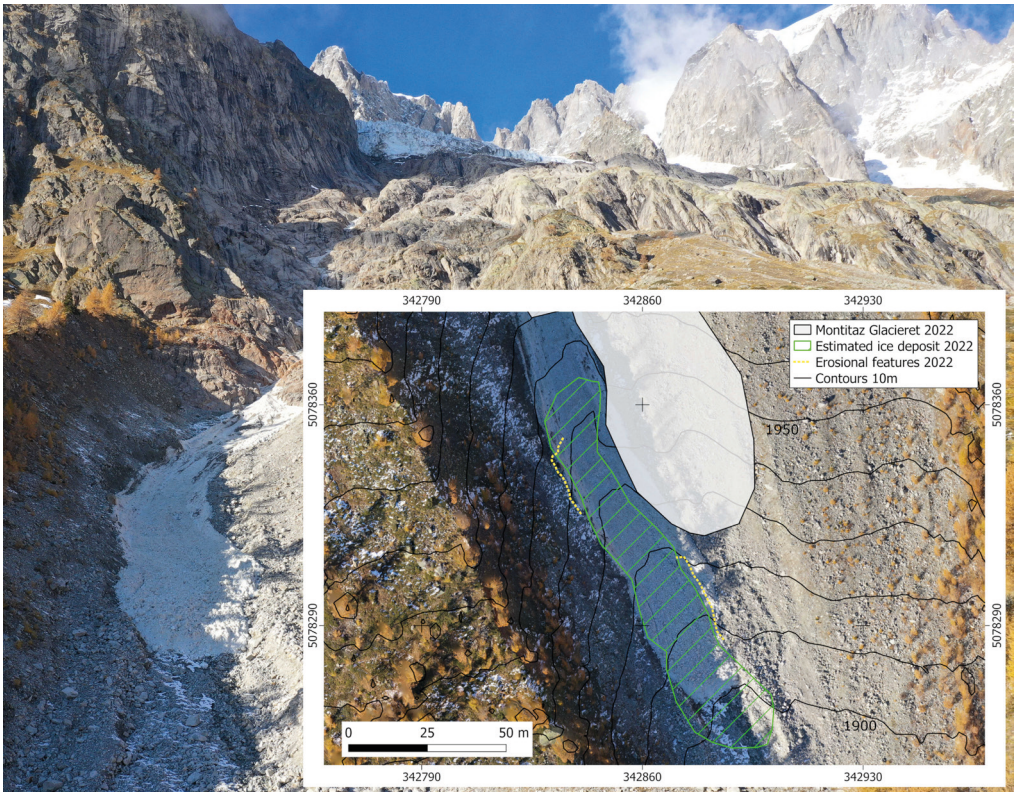

FIG. 9 - Oblique image (main panel) and orthoimage (inset) of the ice avalanche of 10th November, 2021. The estimated ice avalanche deposition of the event of 23 June, 2022 is overlayed in green for comparison. The location of the erosional features originated by the 23 June, 2022 event is highlighted in yellow.

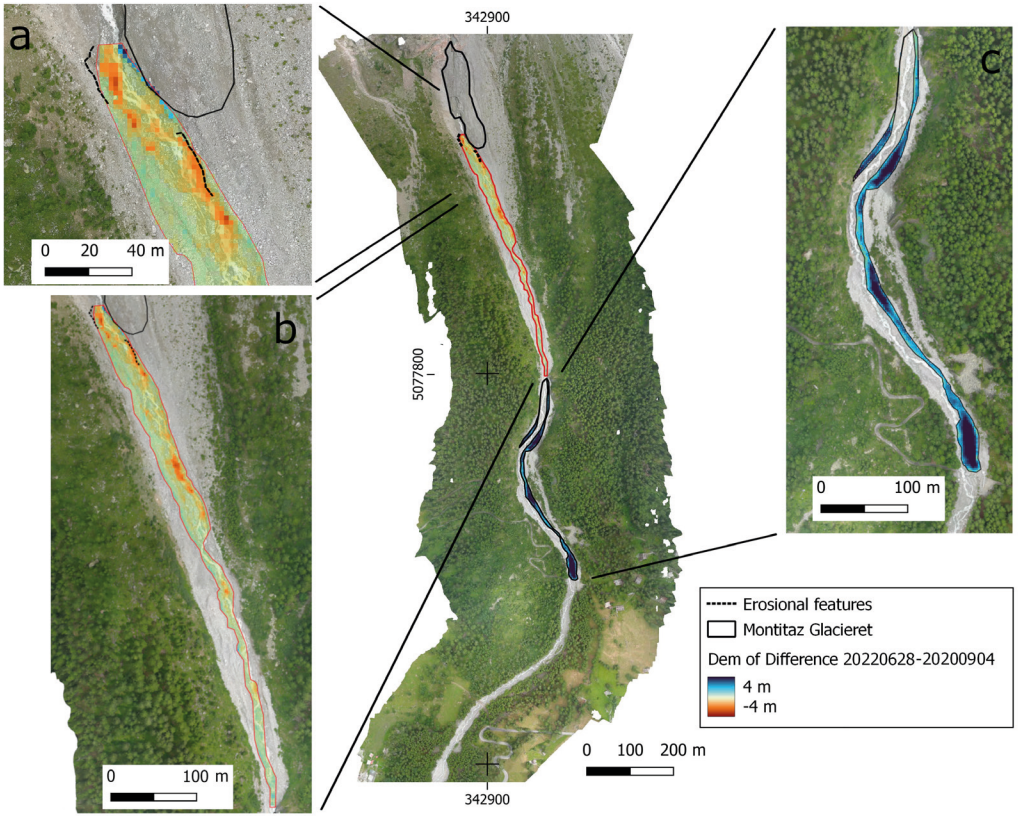

FIG. 10 - Map of the cascading process. The colours indicate the DEM differencing before and after the debris flow (04 September, 2020 – 28 June, 2022). Background: orthoimage of 28 June, 2022. Details of: a) the starting area which caused the remobilisation of the ice debris, b) the erosional area and c) the depositional area along the Montitaz Stream.

DISCUSSION

In this paper, we present a cascade process: a debris flow in the Montitaz Stream that was so intense as to be able to destroy the Rochefort bridge occurred without significant rainfall. In glacial streams, the occurrence of debris flows can be linked to a GLOF or other events that can trigger these potentially destructive phenomena (Allen & *alii*, 2022). The study of the activation of this event can be beneficial for better comprehension of the sequence of events that concurred with its arising. The presence of the Planpincieux Glacier monitoring network, one of the most complex installed in Italy and in the Alps, allowed us to collect a significant dataset by different instruments.

The multi-source dataset has been fundamental to reconstruct the state of the involved elements: Planpincieux glacier, glacieret and Montitaz stream – before the cascading process as follows:

– a large deposit of ice – the Montitaz Glacieret – is present at the top of the glacial fan, fed by the intense calving activity of the Planpincieux glacier in 2022;
– the presence of the glacieret facilitates longer runouts of relatively small ice avalanches due to the reduced friction of the ice;
– the water discharge that alimented the Montitaz Stream from the Planpincieux glacier is abundant due to the high temperatures of the warm season.

The early activation of the ice avalanching processes at Planpincieux Glacier, although still not completely understood, could be linked to high temperatures in the spring period. This would enhance snow melt and cause an increase in basal water pressure at the ice-bedrock interface that decreases basal friction and determines strong accelerations and fracturations in the ice mass. These conditions are prone to the formation of large ice avalanches detaching from the glacial front.

The sequence of events that have been documented on the day of the event is:

i) a limited rainfall event (~6.5 mm) happened in the previous 24 hours and was mostly concentrated between h 14:00 and h 15:00;
ii) an ice avalanche (~4200 m^3) broke off from the Planpincieux Glacier between h 18:00 and h 19:00, impacted on the Montitaz Glacieret and moved further downstream it;
iii) a debris flow damaged the bridge on the Montitaz Stream at h 20:47;

Therefore, the probable dynamics of the cascading process is the following: the ice avalanche deposit formed an unstable ice dam just downstream from the glacieret. The input provided by the Montitaz Stream caused water accumulation above the dam for approximately one to two hours. Subsequently, the dam collapsed. Then, water, ice debris and morainic material were released abruptly, triggering a debris flow. Flowing downstream, the debris flow entrained more debris from the glacial fan and reached the Planpincieux-Rochefort road, damaging the bridge and filling the riverbed with up to 6 m of debris deposit (fig. 11).

We obtained this reconstruction of the occurred events after considering all possible solutions. Alternative causes that might have generated the debris flow are: i) liquid precipitation alone, without the involvement of any glacial component; ii) a GLOF starting from the Planpincieux Glacier; iii) a partial collapse of the Montitaz Glacieret.

The first case is highly improbable because the cumulated precipitation and intensity were very limited and concentrated several hours before the debris flow, as shown in fig 5. The distribution of precipitations excluded a direct impact in the debris flow trigger.

The second case – a GLOF from the main glacier – is also unlikely, because similar phenomena have already been observed in the Planpincieux Glacier, and they leave typical cavities that are easily recognisable on high-resolution time-lapse photography (Giordan & *alii*, 2020). But, in this case, nothing similar was noticed nor registered by the doppler radar and the AXIS camera.

Finally, we also excluded the hypothesis of a partial collapse of the Montitaz Glacieret for two reasons: 1) we did not notice morphological variations of the glacieret terminus on the images of the AXIS camera after the event; and 2) the starting point of the debris flow corresponded exactly with the terminal part of the glacieret, as delineated on the NDWI maps less than 10 hours before the debris flow. Therefore, there was no evidence of a collapse of a substantial portion of the glacieret.

Based on our estimations of the mobilised volumes of material involved in the event of 23 June, 2022, an imbalance in the eroded vs deposited material can be noted. The main cause of the difference probably relies in the fact that the most recent DEM available for representing the pre-event status, although relatively recent, dates back to September 2020, almost two years before the event. Even if two years seems a long timespan for such a stream to preserve its morphology, this was the most recent data available to analyse the phenomena. This implies that we are missing any depositional or erosional event or process that could have happened from September 2020 to June 2022 (Roelofs & *alii*, 2022; Walter & *alii*, 2022). Therefore, we believe that depositional processes in the upper part of the stream played a significant role in the surplus of the depositional part in our calculations. The reason resides mostly in the fact that the debris fan of the Montitaz Stream is very active, both for snow avalanche activity during the winter and ice avalanche activity during the summer. UAV surveys of the area frequently showed macroscopic presence of rock debris in the ice avalanches deposits. This is normal because of the cirque morphology of the Planpincieux Glacier, surrounded by massive rock walls that are affected by frequent rock falls (some larger rock avalanches have also been documented on the glacier surface by the monitoring network in the past). The cumulated ice avalanche volume that falls from the Planpincieux Glacier front onto the Montitaz debris fan during an entire season can reach hundreds of thousands of cubic meters easily (in 2020, a total of 350,000 m^3 was estimated). Estimating a rough debris content of 0.5% in volume of the glacier ice (Hunter & *alii*, 1996; Miles & *alii*, 2021), the order of magnitude of the subsequent deposition from an entire season of ice avalanche activity falls in the range of the missing eroded volume that we noticed in our estimations.

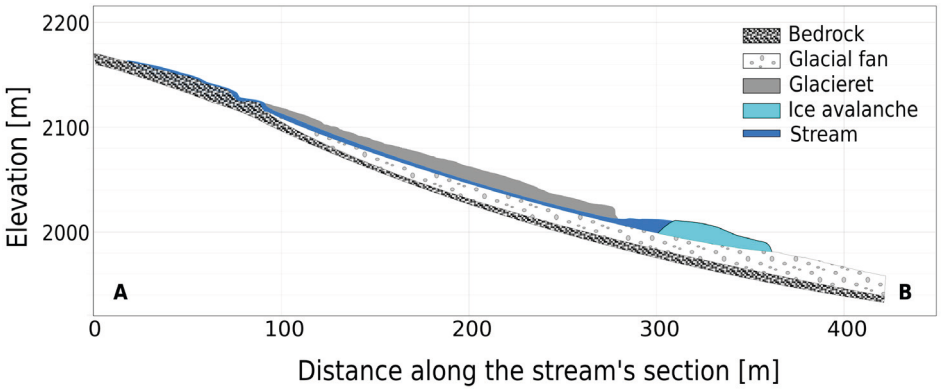

FIG. 11 - Conceptual model of the event triggering mechanism. The thickness of the glacieret and the ice avalanche are magnified for better reading.

Ice avalanches from the glacier front of the Planpincieux Glacier are frequent in summer, but the accumulations of ice avalanche debris seldom generate hydraulic problems on the Montitaz stream; in this frame, it would be possible to think that some particular conditions could have contributed to the triggering of the described event.

In the last decade, every year has shown a period of stronger ice fall activity in the summer season. Still, some years have shown larger cumulated ice avalanche accumulation, like 2020, with an estimated total of 350,000 m^3. In the years that showed less ice fall activity, like 2014, we estimated a cumulated ice avalanche accumulation of around 100,000 m^3. During the whole season of strong glacial activity, most ice volume falls in smaller events, typically falling in volume of 100-500 m^3. Ice avalanche that fall between 2000-10,000 m^3 normally range from 1 to 5 events per years. Ice fall volumes above 25,000 m^3 have been documented only once in the last 10 years.

In the mid of summer, shorter runouts of ice avalanches are noticed at Planpincieux Glacier. The total disappearance of snow patches from the gully where the ice avalanches flow and smaller extents of the Montitaz Glacieret that are normally observed, are the probable cause of such observations. The consequence is that larger release volumes of ice are needed in mid-summer conditions to reach the Montitaz Glacieret and the Montitaz Stream. Release volumes of 2000-3000 m^3 have been documented to have stopped along the bedrock gully above the Montitaz Glacieret.

In the frame of these observations, we can assess that even though ice avalanches phenomena from the Planpincieux Glacier front are recurrent, the conditions that a large enough ice avalanche is released (order of magnitude of more than 3000-4000 m^3), the Montitaz Stream is not covered by snow avalanche deposits and it has a certain amount of water flowing along its riverbed, are seldom met.

It should also be noted that a certain volume range could be more prone to generate instability and consequent debris flows: a few hundred of cubic meters of ice would not be enough to start a debris flow, but on the other hand a large accumulation of tens of thousands of cubic meters would be difficult to be saturated with water and become unstable.

Even though such a complex event was impossible to be predicted before its happening, and a certain degree of randomness in such events should be accepted, the aim of the study is to better understand hydro-geological risk of mountain environment in the present climate change scenarios; glacial and periglacial areas should be carefully taken into account as potential sources for gravitational phenomena involving ice, snow, debris and/or water by administrations, policy makers and mountain communities.

CONCLUSIONS

This study shows that detailed field surveys and the acquisition of remotely sensed data are needed to correctly describe phenomena originating in complex environments such as high alpine terrain. The availability of a complex monitoring system allowed us to collect a very detailed dataset that supported the reconstruction of an elaborate sequence of events that concur to activating a debris flow without significant rainfalls. The possible activation of a GLOF pushed us to study this event to detect all the possible evidence of this phenomenon. The analysis did not support this possibility but suggested a more complex and unusual sequence of events. The presence of a glacieret modified the behaviour of the ice avalanche and extended its runout. This combination augmented the capacity of water retention and increased the water volume at the moment of the dam break that triggered the debris flow.

The reconstruction of the series of events that led to the formation of this destructive debris flow was possible thanks to the existence of a permanent monitoring network that implements high-rate monitoring systems. A series of further analyses was carried out in this study, but we underline that without the basic inputs from the monitoring network, the reconstruction of the phenomena as a GLOF would have been very likely.

This reconstruction can be useful for the future because some events could be classified as not dangerous if considered independently. Still, when considering the possibility of cascading events, a likelihood of reaching zones at risk could arise. Therefore, knowledge about these processes should increase, and field data should be collected to correctly feed models for the simulation of such phenomena and a possible application of those in the forecast of impacts. Risk management plans should include an evaluation of the possibility of the development of chain processes originating from a single gravitational mass movement.

REFERENCES

Allen S., Frey H., Haeberli W., Hugge C., Chiarle M. & Geertsema M. (2022) - *Assessment principles for glacier and permafrost hazards in mountain regions.* In: Oxford Research Encyclopedia of Natural Hazard Science, Oxford University Press, USA. doi: 10.1093/acrefore/9780199389407.013.356

Berthier E., Vincent C., Magnússon E., Gunnlaugsson Á.Þ., Pitte P., Le Meur E., Masiokas M., Ruiz L., Pálsson F., Belart J.M.C. & Wagnon P. (2014) - *Glacier topography and elevation changes derived from Pléiades sub-meter stereo images*. The Cryosphere, 8 (6), 2275-2291.

Caduff R., Schlunegger F., Kos A. & Wiesmann A. (2015) - *A review of terrestrial radar interferometry for measuring surface change in the geosciences.* Earth Surface Processes and Landforms, 40 (2), 208-228.

Carrivick J.L. & Tweed F.S. (2016) - *A global assessment of the societal impacts of glacier outburst floods*. Global and Planetary Change, 144, 1-16.

Cicoira A., Blatny L., Li X., Trottet B. & Gaume J. (2022) - *Towards a predictive multi-phase model for alpine mass movements and process cascades*. Engineering Geology, 310, 106866.

Cuffey K.M. & Paterson W.S.B. (2010) - *The Physics of Glaciers*. Academic Press, Oxford, 704 pp.

Dematteis N., Giordan D., Troilo F., Wrzesniak A. & Godone D. (2021) - *Ten-year monitoring of the Grandes Jorasses Glaciers kinematics. Limits, potentialities, and possible applications of different monitoring systems*. Remote Sensing, 13 (15), 3005.

Emmer A. (2017) - *Glacier retreat and glacial lake outburst floods (GLOFs).* In: Oxford Research Encyclopedia of Natural Hazard Science, Oxford University Press, USA. doi: 10.1093/acrefore/9780199389407.013.275

Emmer A., Allen S.K., Carey M., Frey H., Huggel C., Korup O., Mergili M., Sattar A., Veh G. & Chen T.Y. (2022) - *Progress and challenges in glacial lake outburst flood research (2017-2021): A research community perspective*. Natural Hazards and Earth System Sciences, 22 (9), 3041-3061.

Evans A.N. (2000) - *Glacier surface motion computation from digital image sequences*. IEEE Transactions on Geoscience and Remote Sensing, 38 (2), 1064-1072.

Giordan D., Allasia P., Dematteis N., Dell'Anes, F., Vagliasindi M. & Motta E. (2016) - *A low-cost optical remote sensing application for glacier deformation monitoring in an alpine environment.* Sensors, 16 (10), 1750.

Giordan D., Dematteis N., Allasia P. & Motta E. (2020) - *Classification and kinematics of the Planpincieux Glacier break-offs using photographic time-lapse analysis*. Journal of Glaciology, 66 (256), 188-202.

Halwas K.L. & Church M. (2002) - *Channel units in small, high gradient streams on Vancouver Island, British Columbia*. Geomorphology, 43 (3-4), 243-256.

Harrison S., Kargel J.S., Huggel C., Reynolds J., Shugar D.H., Betts R.A., Emmer A., Glasser N., Haritashya U.K., Klimeš J., Reinhardt L., Schaub Y., Wiltshire A., Regmi D. & Vilímek V. (2018) - *Climate change and the global pattern of moraine-dammed glacial lake outburst floods.* The Cryosphere, 12 (4), 1195-1209. doi: 10.5194/tc-12-1195-2018

Huggel C., Giráldez C., Haeberli W., Schneider D., Frey H., Schaub Y., Cochachin A., Portocarrero C., García J. & Guillén Ludeña S. (2013) - *Climatic extreme events combine with impacts of gradual climate change: recent evidence from the Andes and the Alps*. EGU General Assembly Conference Abstracts.

Hunter L.E., Powell R.D. & Lawson D.E. (1996) - *Flux of debris transported by ice at three Alaskan tidewater glaciers*. Journal of Glaciology, 42 (140), 123-135.

Jebur A., Abed F. & Mohammed M. (2018) - *Assessing the performance of commercial Agisoft PhotoScan software to deliver reliable data for accurate 3D modelling*. MATEC Web of Conferences,

Kääb A., Reynolds J.M. & Haeberli W. (2005) - *Glacier and permafrost hazards in high mountains*. In: Huber U.M., Bugmann H.K.M. & Reasoner M.A. (Eds.), Global change and mountain regions: An overview of current knowledge, 225-234. Springer, Dordrecht.

Mazzorana B., Picco L., Rainato R., Iroumé A., Ruiz-Villanueva V., Rojas C., Valdebenito G., Iribarren-Anacona P. & Melnick D. (2019) - *Cascading processes in a changing environment: Disturbances on fluvial ecosystems in Chile and implications for hazard and risk management*. Science of the Total Environment, 655, 1089-1103.

McFeeters S.K. (1996) - *The use of the Normalized Difference Water Index (NDWI) in the delineation of open water features*. International Journal of Remote Sensing, 17 (7), 1425-1432.

Meier L., Jacquemart M., Blattmann B. & Arnold B. (2016) - *Real-time avalanche detection with long-range, wide-angle radars for road safety in Zermatt, Switzerland*. Proceedings of the International Snow Science Workshop, Breckenridge, Colorado, 304-308.

Mergili M., Jaboyedoff M., Pullarello J. & Pudasaini S.P. (2020) - *Back calculation of the 2017 Piz Cengalo–Bondo landslide cascade with r.avaflow: What we can do and what we can learn*. Natural Hazards and Earth System Sciences, 20 (2), 505-520.

Miles K.E., Hubbard B., Miles E.S., Quincey D.J., Rowan A.V., Kirkbride M. & Hornsey J. (2021) - *Continuous borehole optical televiewing reveals variable englacial debris concentrations at Khumbu Glacier, Nepal*. Communications Earth & Environment, 2 (1), 12.

Monserrat O., Crosetto M. & Luzi G. (2014) - *A review of ground-based SAR interferometry for deformation measurement*. ISPRS Journal of Photogrammetry and Remote Sensing, 93, 40-48.

Nuth C. & Kääb A. (2011) - *Co-registration and bias corrections of satellite elevation data sets for quantifying glacier thickness change*. The Cryosphere, 5 (1), 271-290.

Pandey V.K., Kumar R., Singh R., Kumar R., Rai S.C., Singh R.P., Tripathi A.K., Soni V.K., Ali S.N. & Tamang D. (2022) - *Catastrophic ice-debris flow in the Rishiganga River, Chamoli, Uttarakhand (India)*. Geomatics, Natural Hazards and Risk, 13 (1), 289-309.

Pralong A. & Funk M. (2006) - *On the instability of avalanching glaciers*. Journal of Glaciology, 52 (176), 31-48.

Roelofs L., Colucci P. & de Haas T. (2022) - *How debris-flow composition affects bed erosion quantity and mechanisms: An experimental assessment*. Earth Surface Processes and Landforms, 47 (8), 2151-2169.

Schneider D., Huggel C., Cochachin A., Guillén S. & García J. (2014) - *Mapping hazards from glacier lake outburst floods based on modelling of process cascades at Lake 513, Carhuaz, Peru*. Advances in Geosciences, 35, 145-155.

Schwalbe E. & Maas H.G. (2017) - *The determination of high-resolution spatio-temporal glacier motion fields from time-lapse sequences*. Earth Surface Dynamics, 5 (4), 861-879.

Walter F., Hodel E., Mannerfelt E.S., Cook K., Dietze M., Estermann L., Wenner M., Farinotti D., Fengler M. & Hammerschmidt L. (2022) - *Brief communication: An autonomous UAV for catchment-wide monitoring of a debris flow torrent*. Natural Hazards and Earth System Sciences, 22 (12), 4011-4018.

Zemp M., Nussbaumer S.U., Gärtner-Roer I., Bannwart J., Paul F. & Hoelzle M. (Eds.) (2021) - *Global Glacier Change Bulletin*, 4 (2018-2019) - World Glacier Monitoring Service, Zurich, Switzerland, 278 pp.

(Ms. received 26 March 2023, accepted 23 June 2023)